

# Sigma-Delta Learning for Super-resolution Independent Component Analysis

Amin Fazel and Shantanu Chakrabartty  
Department of Electrical and Computer Engineering  
Michigan State University  
East Lansing, Michigan 48824-1226  
Email: {fazel, shantanu}@egr.msu.edu

**Abstract**—Many source separation algorithms fail to deliver robust performance in presence of artifacts introduced by cross-channel redundancy, non-homogeneous mixing and high-dimensionality of the input signal space. In this paper, we propose a novel framework that overcomes these limitations by integrating learning algorithms directly with the process of signal acquisition and sampling. At the core of the proposed approach is a novel regularized max-min optimization approach that yields “sigma-delta” limit-cycles. An on-line adaptation modulates the limit-cycles to enhance resolution in the signal sub-spaces containing non-redundant information. Numerical experiments simulating near-singular and non-homogeneous recording conditions demonstrate consistent improvements of the proposed algorithm over a benchmark when applied for independent component analysis (ICA).

## I. INTRODUCTION

Separation or recovery of sources of interest within high-dimensional data constitutes a fundamental problem in neural network research [1], [2]. Most source separation algorithms reported in literature operate by learning parameters of a linear or non-linear transformation that projects the high-dimensional data onto a linear or a non-linear manifold while preserving or optimizing some topological (distance) or statistical property of the data. Some of the examples include principal component analysis [3], independent component analysis [4], [5], factor analysis [6], and projection pursuit [7] that have been successfully applied to different areas of science and engineering. Independent component analysis belongs to a class of source separation algorithms where the objective is to recover signals or factors that are statistically independent with respect to each other [4], [8]. Since its inception [9], different variants of ICA algorithms have been proposed based on the notion of statistical independence [10], [11]. In their classical setting, ICA and other source separation algorithms are formulated independent of the signal measurement process (analog-to-digital process) and therefore they do not consider the detrimental effects of finite resolution on the performance of the learning algorithm. However, in the case of micro/nano-scale microphone arrays, the mutual dependency of signal measurement and the learning algorithms can not be ignored due to the following reasons:

- **Far-field effects:** Distance between recording elements on the array is much smaller than the distance of the

sources to the sensor array. As a result, the mixing of signals at the sensors is near singular.

- **Near-far effects:** A stronger source that is nearer to the sensor array can completely mask weak background sources.
- **High-dimensionality** of input analog signals due to high integration density of the microphones.

Overcoming these artifacts would require super-resolution processing of the high-dimensional analog space such that acute differences between input signals. In signal processing and circuits community,  $\Sigma\Delta$  modulation have been the de-facto choice for designing high-resolution analog-to-digital converters [12]. In fact resolution greater than 16 bits (greater than 100dB dynamic range) is common for sigma-delta ADCs [12]. Therefore, capturing the dynamics of sigma-delta modulation within the context of statistical learning theory could provide cues for constructing learning algorithms that can process signals at resolutions demanded by high-density arrays. The core principle of the proposed learning algorithm is depicted using Figure 1 which shows a typical distribution for a two-dimensional signal acquired through a high-density array. It can be seen in Figure 1(a) that the distribution is near singular and that the measurements  $x_1$  and  $x_2$  show high-degree of correlation. Our approach is to first determine a quantized representation of a transformation matrix  $\mathbf{W}$ , that will align the data distribution along the orthogonal axes, each representing an independent component (shown in Figure 1(b)). Based on this alignment, the scale of the quantization operation will be adjusted along each of the axes such that all the quantization levels (represented by ticks) span the information bearing region of the signal space at super-resolution scales (Figure 1(c)).

## II. $\Sigma\Delta$ LEARNING

In this section we describe a generalized form of the max-min optimization framework introduced in [13] that unified statistical learning with  $\Sigma\Delta$  modulation. Given a random input vector  $\mathbf{x} \in \mathcal{R}^M$  and an internal state vector  $\mathbf{v} \in \mathcal{R}^M$ , a  $\Sigma\Delta$  learner estimates the parameter of a linear transformation matrix  $\mathbf{W} \in \mathcal{R}^M \times \mathcal{R}^M$  according to the following optimization criterion:

$$\max_{\mathbf{W} \in \mathcal{C}} (\min_{\mathbf{v}} C(\mathbf{v}, \mathbf{W})) \quad (1)$$

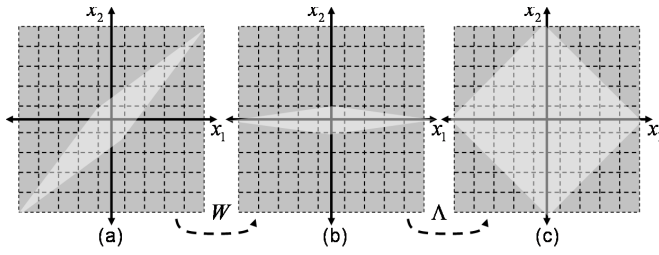


Fig. 1. Illustration of the proposed approach: (a) input signal distribution, (b) signal transformation and (c) resolution enhancement

where

$$C(\mathbf{v}, \mathbf{W}) = \Omega(\mathbf{v}) - \mathbf{v}^T E_{\mathbf{x}}\{\mathbf{W}^T \mathbf{x}\}. \quad (2)$$

$E_{\mathbf{x}}\{\cdot\}$  denotes an expectation operator with respect to the random variable  $\mathbf{x}$ .  $\mathcal{C}$  denotes a constraint space of the transformation matrix  $\mathbf{W}$ .  $\Omega(\cdot)$  is a piece-wise linear regularization function that will be used for implementing quantization operators. This is illustrated in Figure 2 which shows examples of one-dimensional regularization functions  $\Omega(\cdot)$ . The piece-wise behavior of  $\Omega(\cdot)$  will lead to discontinuous gradients  $\nabla\Omega$  (shown in Figure 2(b)) which are equivalent to functions used for signal quantization. The minimization step in equation (1) will ensure that the state vector  $\mathbf{v}$  is correlated with the transformed input signal  $\mathbf{W}\mathbf{x}$  (tracking step) and the maximization step in (1) will adapt the parameters  $\mathbf{W}$  such that it minimizes the correlation (de-correlation step). The formulation bears similarities with game-theoretic approaches where tracking and de-correlation have been formulated as conflicting objectives. The uniqueness of the proposed approach, compared to other optimization techniques to solve (1) is the use of bounded gradients to generate  $\Sigma\Delta$  limit-cycles. This is shown in Figure 3 which illustrates the proposed optimization procedure using a two-dimensional contour. Provided the input  $\mathbf{x}$  and the norm of the linear transformation  $\|\mathbf{W}\|_{\infty}$  are bounded and the regularization function  $\Omega$  satisfies the Lipschitz condition, the optimal solution to (1) is well defined and is given by  $\mathbf{v}^* = 0$  (see Figure 3). In the proposed approach, however, only the path to the final solution  $\mathbf{v}^*$  and the limit-cycles about the solution (see Figure 3) will be of importance. The path and the limit-cycles will encode the topology of the optimization manifold which is defined by input vector  $\mathbf{x}$  and the transformation  $\mathbf{W}$ .

#### A. $\Sigma\Delta$ Modulation

The link between optimization (1) and  $\Sigma\Delta$  modulation is the minimization operation in (1) where a stochastic gradient descent step yields

$$\mathbf{v}_n = \mathbf{v}_{n-1} + \mathbf{W}_n^T \mathbf{x}_n - \mathbf{d}_n \quad (3)$$

with  $n$  signifying the time steps and  $\mathbf{d}_n = \nabla\Omega(\mathbf{v}_{n-1})$  being the quantized representation according to functions shown in Figure 2. Note that the formulation (3) does not require any learning rate parameters typically used in other neural network approaches. As the recursion (3) progresses, bounded limit

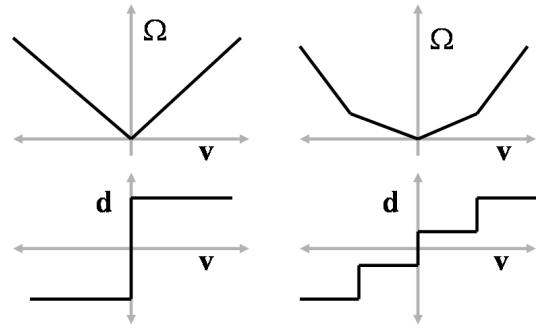


Fig. 2. One dimensional piece-wise linear regularization functions (a) two level (b) multi-level

cycles are produced about the solution  $\mathbf{v}^*$  (see Figure 3). It can be shown that for  $\|\mathbf{W}_n\|_{\infty} \leq 1$  then  $\|\mathbf{v}_n\|_{\infty} \leq 1$ , which leads to  $E_n\{\mathbf{d}_n\} \xrightarrow{n \rightarrow \infty} E_n\{\mathbf{W}_n \mathbf{x}_n\}$ , where  $E_n\{\cdot\}$  denotes an empirical expectation with respect to time indices  $n$ . Thus, recursion (3) produces a quantized sequence whose mean asymptotically encodes the transformed input at infinite resolution. For a stationary input source,  $\mathbf{W}_n$  converges to an asymptotic value  $\mathbf{W}_{\infty}$ , which then can be used for reconstruction according to  $E_n\{\hat{\mathbf{x}}_n\} \approx \mathbf{W}_{\infty}^{-1} E_n\{\mathbf{d}_n\}$ , where  $\mathbf{W}_{\infty}^{-1}$  is the inverse transform. The constraint space  $\mathcal{C}$  could be therefore chosen such that the inverse transform always exists. An example of such a constraint space is a set of lower or upper triangular matrices whose diagonal elements are fixed.

#### B. $\Sigma\Delta$ decorrelation

The maximization step (de-correlation) in equation (1) yields updates for matrix  $\mathbf{W}$  according to:

$$\mathbf{W}_n = \mathbf{W}_{n-1} - 2^{-P} \mathbf{d}_n \psi(\mathbf{x}_n)^T; \mathbf{W}_n \in \mathcal{C} \quad (4)$$

where  $\psi: \mathcal{R}^M \rightarrow \mathcal{R}^M$  function dependent on the transformation  $\mathbf{W}$ . For instance,  $\psi(\cdot)$  could be chosen to be a quantized function which yields a completely digital update for (4).  $P$  in equation (4) is an update parameter which determines the resolution of the parameter matrix  $\mathbf{W}$ . In this paper, we have chosen  $\psi(\mathbf{x}_n) = \mathbf{d}_n$  and the constraint space  $\mathcal{C}$  has been chosen to restrict  $\mathbf{W}$  to be a lower triangular matrix with all diagonal elements to be unity. The choice of this constraint guarantees convergence of the updates (3) and (4). It can be seen from the equation (4) that if  $\|\mathbf{W}\|_{\infty}$  is bounded, recursion (4) will asymptotically lead to  $E_n\{\mathbf{d}_n \mathbf{d}_n^T\} \rightarrow \mathbf{0}$  for  $\mathbf{W}_{\infty} \in \mathcal{C}$ . Thus, the proposed  $\Sigma\Delta$  learning algorithm produces quantized sequences that are mutually orthogonal.

#### C. $\Sigma\Delta$ Resolution Enhancement

One of the advantages of integrating signal de-correlation and dimensionality reduction with the analog-to-digital conversion is the ability to enhance the overall resolution of the system by “zooming” into the transformed signal space that contains low energy (for example dimension  $x_2$  in Figure 1(b)). This feature is essential for normalizing the signal power of independent sources, especially when one of the

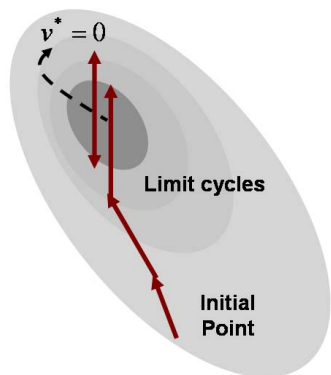


Fig. 3. Limit cycle behavior using bounded gradients

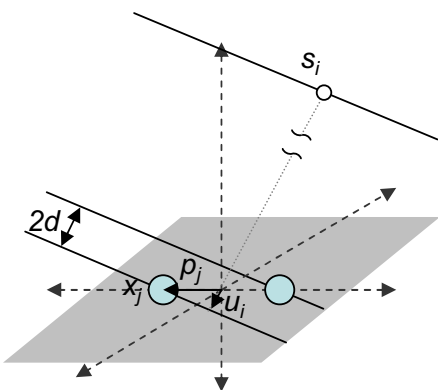


Fig. 4. Far-field recording on a miniature microphone array

sources is masked by another dominant source or common-mode interference. The “zoom” mechanism can be incorporated by introducing a diagonal matrix  $\Lambda \in \mathcal{R}^M \times \mathcal{R}^M$  into the cost function (2) as

$$C(\mathbf{v}, \mathbf{W}, \Lambda) = \Omega(\Lambda^T \mathbf{v}) - \mathbf{v}^T E_{\mathbf{x}} \{ \mathbf{W}^T \mathbf{x} \}. \quad (5)$$

where the optimization (1) is also performed with respect to the parameter matrix  $\Lambda$ . The stochastic gradient step equivalent to recursion (3) is given by

$$\mathbf{v}_n = \mathbf{v}_{n-1} + (\mathbf{W}_{n-1}^T \mathbf{x}_n - \Lambda_n^T \mathcal{D}_n) \quad (6)$$

The asymptotic behavior of update (6) for equation (5) can be expressed as  $E_n \{ \mathcal{D}_n \} \xrightarrow{n \rightarrow \infty} \Lambda^{-1} E_n \{ \mathbf{W}_n^T \mathbf{x}_n \}$ . Thus reducing the magnitude of diagonal matrix  $\Lambda$  will result in an equivalent amplification of the transformed signal. The parameter  $\Lambda$  is determined based on the following element-wise update

$$\Lambda_i = \max |(\mathbf{W}_n \mathbf{x}_n)_i|; n > N_0 \quad (7)$$

which ensures that the updates (6) and (7) are always bounded.

### III. APPLICATION OF $\Sigma\Delta$ LEARNING FOR FAR-FIELD SOURCE SEPARATION

In literature far-field acoustics have been extensively studied within context of array processing [14], [15] and plenacoustic

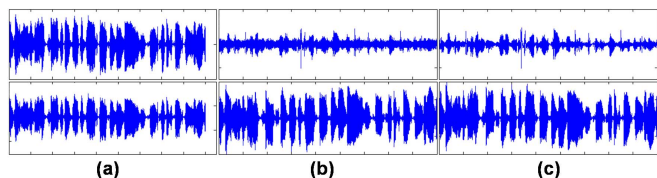


Fig. 5. Speech signals corresponding to: (a) recording at each of the two microphones, (b) sources recovered after applying fastICA to an 8 bit ADC (c) sources recovered by an 8 bit  $\Sigma\Delta$  learner and fastICA

models [16]. We concisely describe a simplistic model that have been previously used for miniature microphone arrays. For audio signals (100-20,000 Hz), microphone arrays with inter-element distances less than  $3.4\text{cm}$  (coherence length) can be approximated by far-field, where the acoustic wavefronts can be considered planar (see Figure 4). Also, for miniature microphone arrays the distance to the acoustic sources from the center of the array can be assumed to be larger than inter-element distance. We express the signal  $x_j(\mathbf{p}_j, t)$  recorded at  $j^{\text{th}}$  microphone located at a 3-D position vector  $\mathbf{p}_j = (x, y, z)$  as a superposition  $i \in 1, \dots, D$  independent sources  $s_i(t)$  recorded at the reference microphone (located at the center of the array) [16]. This can be written as

$$x_j(\mathbf{p}_j, t) = \sum_i c_i(\mathbf{p}_j) s_i(t - \tau_i(\mathbf{p}_j)) \quad (8)$$

where  $c_i(\mathbf{p}_j)$  and  $\tau_i(\mathbf{p}_j)$  are the attenuation and delay, relative to the center of microphone array, for the source  $s_i(t)$  at the position  $\mathbf{p}_j$ . Under far-field conditions it can be assumed that  $c_i(\mathbf{p}_j) \approx 1$  and  $\tau_i(\mathbf{p}_j) \ll t$ . Similar other treatments, equation (8) can be approximated using Taylor’s series expansion as

$$x_j(\mathbf{p}_j, t) \approx \sum_i s_i(t) - \sum_i \tau_i(\mathbf{p}_j) \dot{s}_i(t). \quad (9)$$

The first right hand part of the equation (9) signifies a common-mode signal and the second part signifies an instantaneous mixture of the derivative of the source signals. Fortunately, for miniature arrays, the time delays can expressed as linear terms as  $\tau_i(\mathbf{p}_j) = \mathbf{u}_i^T \mathbf{p}_j / c$ , where  $\mathbf{u}_i$  is the unit normal vector of the wavefront of source  $i$ . For distance of  $j^{\text{th}}$  microphone from reference position  $|d|_{\min} = \mathbf{u}_i^T \mathbf{p}_j = 1\text{mm}$ ,  $c = 340\text{m/s}$  and signal frequency of  $1000\text{Hz}$ , any signal processor has to resolve signals less than  $-70\text{dB}$  relative to the common-mode. Figure 5(a) shows a sample recording for a two microphone array when the placement between the recording elements is  $1\text{cm}$ .

For our experiments we simulated a recording conditions of a miniature array consisting of 4 omni-directional microphones. Three of the microphones were placed along a triangle with distance being  $1\text{mm}$ , whereas the fourth microphone was placed at the centroid. The set up is similar to the conditions that have been reported in [15] where the simulation have been shown to closely approximate real-life anechoic conditions. To simulate microphone and amplifier noise wide-band noise were added to each of the mixed sources. Also, the simulations

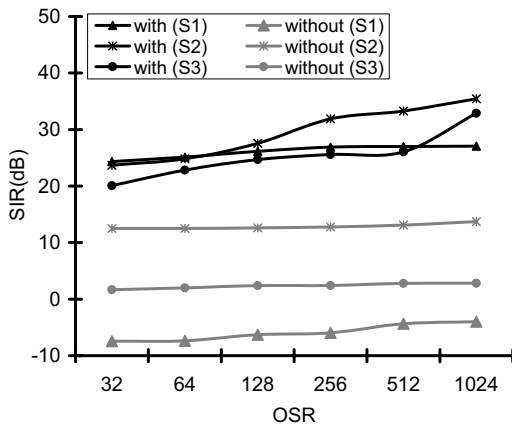


Fig. 6. Comparative study for different  $\Sigma\Delta$  over-sampling ratio

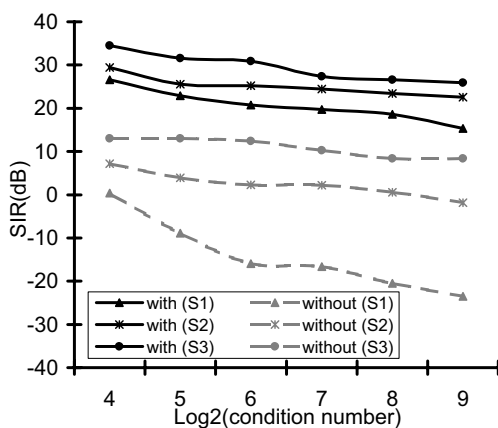


Fig. 7. Comparative study for different mixing conditions quantified by its condition number.

were performed assuming up to 5% mismatch in the gain of the microphones. For all experiments three independent speech signals were chosen as far-field sources and the location of the sources were varied to generate different mixing conditions at the microphone array. The outputs of the microphone array were first presented to the proposed  $\Sigma\Delta$  learner, subsequent to which, only three of the outputs are used as inputs to the FastICA algorithm [4]. A benchmark used for comparative study consisted of  $\Sigma\Delta$  converters which directly quantized the mixtures recorded at the four microphones. Figures 5(b) and (c) show the recovered speech signal when FastICA algorithm was applied to an eight bit quantized signal and when FastICA algorithm is applied subsequent proposed  $\Sigma\Delta$  learning algorithm operating at an oversampling ratio of 256 (8 bits). The quality of separation produced by the proposed algorithm and its benchmark have been compared using signal-to-interference ratio (SIR) and signal-to-distortion ratio [17] which takes into account degradation due to noise and cross-channel leakage.

The experimental results are summarized by Figure 6 and

Figure 7, where the SIR is computed for each of the sources (S1-S3) for different values of oversampling ratio  $N$ , and for different placement of far-field sources (quantified using the condition number of the mixing matrix). In both the cases, the proposed  $\Sigma\Delta$  learner (denoted by “with”) outperforms its benchmark (denoted by “without”) which completely fails to resolve acute differences between microphone signals for different over-sampling ratio and for near singular mixing (large condition number).

#### IV. CONCLUSION

In this paper, we have proposed a novel framework that integrates machine learning with analog-to-digital conversion. One of the applications of this integration is the ability to resolve acute differences in signals recorded using a miniature microphone array where classical approach of digitization followed by source separation fails to produce robust results. Using numerical simulations we have shown that the framework demonstrates consistent improvements in performance over a benchmark system when applied for independent component analysis.

#### REFERENCES

- [1] S. Haykin, *Neural Networks: A comprehensive foundation*, 2nd ed. Upper Saddle River NJ: Prentice Hall PTR, 1998.
- [2] C. M. Bishop, *Neural Networks for Pattern Recognition*, Oxford: Oxford University Press, 1995.
- [3] I. T. Jolliffe, *Principal Component Analysis*, 2nd ed. New York: Springer, 2002.
- [4] A. Hyvärinen, J. Karhunen, and E. Oja, *Independent Component Analysis*, New York: Wiley, 2001.
- [5] A. Cichocki and S. Amari, *Adaptive blind signal and image processing: learning algorithms and applications*, New York: Wiley, 2002.
- [6] R. L. Gorsuch, *Factor Analysis*, 2nd ed. Hillsdale NJ: Erlbaum, 1983.
- [7] P. J. Huber, “Projection Pursuit,” *The Annals of Statistics*, vol. 13, no. 2, pp. 435-475, 1985.
- [8] P. Comon, “Independent component analysis, a new concept?,” *Signal Processing*, vol. 36, no. 3, pp. 287-314, 1994.
- [9] C. Jutten, and J. Héroult, “Blind separation of sources, part I: An adaptive algorithm based on neuromimetic architecture,” *Signal Processing*, vol. 24, no. 1, pp. 1-10, 1991.
- [10] A. J. Bell and T. J. Sejnowski, “An Information Maximization Approach to Blind Separation and Blind Deconvolution,” *Neural Computation*, vol. 7, no. 6, pp. 1129-1159, 1995.
- [11] S. Amari, A. Cichocki, and H. H. Yang, “A new learning algorithm for blind signal separation,” *Advances in Neural Information Processing Systems*, vol. 8, pp. 757-763, MIT Press, Cambridge, MA, 1996.
- [12] S. R. Norsworthy, R. Schreier, and G. C. Temes, *Delta-Sigma Data Converters: Theory, Design, and Simulation*, New York: Wiley-IEEE Press, 1996.
- [13] A. Gore and S. Chakrabarty, “Large Margin Multi-channel Analog-to-Digital Conversion with Applications to Neural Prosthesis,” *Advances in Neural Information Processing Systems*, vol. 19, pp. 497-504, MIT Press, Cambridge, MA, 2007.
- [14] A. Celik, M. Stanacevic, and G. Cauwenberghs, “Gradient flow independent component analysis in micropower VLSI,” *Advances in Neural Information Processing Systems*, vol. 18, pp. 187-194, MIT Press, Cambridge, MA, 2006.
- [15] G. Chabriel, J. Barrère, “An Instantaneous Formulation of Mixtures for Blind Separation of Propagating Waves,” *IEEE Trans. Signal Processing*, vol. 54, no. 1, pp. 49-58, 2006.
- [16] M. N. Do, “Toward sound-based synthesis: the far-field case,” *Proc. of IEEE Intl. Conf. on Acoustics, Speech, and Signal Processing*, Montreal, Canada, May 2004.
- [17] E. Vincent, R. Gribonval, and C. Févotte, “Performance measurement in Blind Audio Source Separation,” *IEEE Trans. Audio, Speech and Language Processing*, vol. 14, no. 4, pp. 1462-1469, 2006.